Molecular Pharmacology Fast Forward. Published on August 10, 2016 as DOI: 10.1124/mol.116.105502
This article has not been copyedited and formatted. The final version may differ from this version.

CXC Chemokine Receptor 3 Alternative Splice Variants Selectively Activate Different Signaling Pathways

Yamina A. Berchiche & Thomas P. Sakmar

Laboratory of Chemical Biology and Signal Transduction, The Rockefeller University, New York, USA (Y.A.B and T.P.S.); Department of Neurobiology, Care Sciences and Society, Division of Neurogeriatrics, Center for Alzheimer Research, Karolinska Institutet, 141 57 Huddinge, Sweden (T.P.S)

Molecular Pharmacology Fast Forward. Published on August 10, 2016 as DOI: 10.1124/mol.116.105502
This article has not been copyedited and formatted. The final version may differ from this version.

Running Title Page

Differential Activation of CXC Chemokine Receptor 3 Splice Variants

Correspondence: Thomas P. Sakmar, Laboratory of Chemical Biology and Signal Transduction, Box 187, RRB 510, 1230 York Ave., New York, NY, USA, 10065.

Email: sakmar@rockefeller.edu

Number of text pages: 40

Number of tables: 3

Number of figures: 8

Number of references: 54

Number of words in abstract: 216

Number of words in introduction: 727

Number of words in discussion: 1465

Non-standard abbreviations: CXCR, CXC chemokine receptor, CXCL, CXC chemokine ligand, GPCR, G-protein-couple receptor, BRET, bioluminescence resonance energy transfer; GFP, Green Fluorescent Protein; RLuc ,*Renilla Reniformis* luciferase, HEK, human embryonic kidney, PTX, pertussis toxin, ERK, Extracellular signal Regulated Kinase, ANOVA, analysis of variance.

Molecular Pharmacology Fast Forward. Published on August 10, 2016 as DOI: 10.1124/mol.116.105502
This article has not been copyedited and formatted. The final version may differ from this version.

Abstract

The G protein-coupled receptor (GPCR) C-X-C chemokine receptor 3 (CXCR3) is a potential drug target that mediates signaling involved in cancer metastasis and inflammatory diseases. The CXCR3 primary transcript has three potential alternative splice variants and cell-type specific expression results in receptor variants that are believed to have different functional characteristics. However, the molecular pharmacology of ligand binding to CXCR3 alternative splice variants, and their downstream signaling pathways, remain poorly explored. To better understand the role of the functional consequences of alternative splicing of CXCR3, we measured signaling in response to four different chemokine ligands (CXCL4, CXCL9, CXCL10 and CXCL11) with agonist activity at CXCR3. Both CXCL10 and CXCL11 activated splice variant CXCR3A. While CXCL10 displayed full agonistic activity for Gαi activation and ERK1/2 phosphorylation, and partial agonist activity for β-arrestin recruitment, CXCL9 triggered only modest ERK1/2 phosphorylation. CXCL11 induced CXCR3B-mediated β-arrestin recruitment and little ERK phosphorylation. CXCR3Alt signaling was limited to modest ligand-induced receptor internalization and ERK1/2 phosphorylation in response to chemokines CXCL11, CXCL10 and CXCL9. These results show that CXCR3 splice variants activate different signaling pathways and that CXCR3 variant function is not redundant, suggesting a mechanism for tissue specific biased agonism. Our data show an additional layer of complexity for chemokine receptor signaling that might be exploited to target specific CXCR3 splice variants.

Molecular Pharmacology Fast Forward. Published on August 10, 2016 as DOI: 10.1124/mol.116.105502
This article has not been copyedited and formatted. The final version may differ from this version.

Introduction

Chemokine receptors are members of the G protein-coupled receptors (GPCR) family that bind peptidic chemotactic cytokines also known as chemokines. One hallmark of chemokine receptors is that they tend to have multiple endogenous agonist ligands. And conversely, some chemokines can activate multiple separate chemokine receptor subtypes. Accumulating *in vitro* and *in vivo* evidence suggests that this promiscuity results in a diversity of specific chemokine receptor signaling, rather than mere functional redundancy (Schall and Proudfoot, 2011). Furthermore, chemokine receptor signaling is also controlled by chemokine binding to proteoglycans (Brady and Limbird, 2002; Groom and Luster, 2011b; Proudfoot et al., 2003; Zweemer et al., 2014), post-translational modifications and chemokine dimerization (Ludeman and Stone, 2014). Another potential mechanism controlling receptor function is the expression of alternative splice variants, which remains poorly explored (Wise, 2012). Since many chemokine receptors and chemokines are co-expressed by the same cell types, or are present in the same cellular environment during inflammation, it is challenging to assess differences in the function of chemokine receptors and their alternative splice variants in response to different ligands in *in vivo* settings.

Inflammatory chemokine receptor CXCR3 is of increasing clinical interest since it controls leukocyte chemotaxis and is involved in inflammatory disorders such as atherosclerosis, as well as in cancer metastasis (Groom and Luster, 2011a; b; Hancock et al., 2000; Li et al., 2015; Lleo et al., 2015; Murphy et al., 2000; Zhu et al., 2015). CXCR3 is expressed at the surface of a plethora of cells, including monocytes, lymphocytes, natural killer and endothelial cells (Garcia-Lopez et al., 2001). CXCR3

Molecular Pharmacology Fast Forward. Published on August 10, 2016 as DOI: 10.1124/mol.116.105502
This article has not been copyedited and formatted. The final version may differ from this version.

displays classic receptor-ligand promiscuity and binds four chemokine ligands: CXCL4, CXCL9, CXCL10 and CXCL11 (Cole et al., 1998; Loetscher et al., 1996; Mueller et al., 2008). CXCR3 couples to Gαi/o heterotrimeric G proteins, which are pertussis toxin (PTX)-sensitive, and can also activate signaling pathways including MAPK, intracellular calcium flux, actin polymerization and chemotaxis in response to chemokines (Kouroumalis et al., 2005; Loetscher et al., 1996; Smit et al., 2003; Thompson et al., 2007). The CXCR3 receptor displays three alternative splice variants. Following the identification of the canonical receptor CXCR3A (Loetscher et al., 1996), two naturally occurring alternative splice variants, CXCR3B and CXCR3Alt, were also identified (Ehlert et al., 2004; Lasagni et al., 2003). Compared with CXCR3A, CXCR3B has an additional 51 amino acids at its N-terminal tail, while CXCR3Alt has a major truncation of intracellular loop three and transmembrane (TM) helices six and seven, which results in a mature protein with possibly only five TM helices and a short cytoplasmic C-terminal tail (Supplementary Figures 1 and 2).

The expression patterns and function of CXCR3 splice variants in normal and disease states remain largely unexplored. Tissue specific expression of CXCR3 alternative variants has been mainly quantified using RT-PCR, and variant-specific antibodies that might allow measurement of expression levels remain unavailable. Nevertheless, in prostate cancer specimens CXCR3A mRNA levels are up regulated while CXCR3B mRNA levels are down regulated (Wu et al., 2012). These differences receptor variant expression levels are reported to alter the migration and invasion capabilities of prostate cancer cells (Wu et al., 2012). In addition, mRNA levels of CXCR3A are decreased while CXCR3Alt mRNA levels are increased in CD3+

Molecular Pharmacology Fast Forward. Published on August 10, 2016 as DOI: 10.1124/mol.116.105502
This article has not been copyedited and formatted. The final version may differ from this version.

peripheral blood lymphocytes in patients suffering from Crohn's disease, suggesting a variant specific role of CXCR3Alt with Crohn's disease (Manousou et al., 2008).

We set out to determine whether CXCR3 alternative splice variants activated different signaling pathways in response to their chemokine ligands. We dissected signaling profiles across multiple pharmacological assays when CXCR3 variants were individually expressed in an HEK293T expression system. We carefully quantitated receptor expression levels and measured chemokine-induced Gαi activity, β-arrestin recruitment, receptor internalization and ERK1/2 phosphorylation to demonstrate that the nature of the activated signaling pathways depends on both the alternative receptor variant and the chemokine tested. For example, nearly all ligands induced CXCR3 internalization, whereas selected ligands induced β-arrestin recruitment in a PTX-insensitive manner, supporting a possible Gαi-independent mechanism of β-arrestin recruitment to CXCR3A and CXCR3B. Moreover, our results strongly suggest that β-arrestin2 is recruited to both CXCR3A and CXCR3B in a ligand-independent manner. In summary, we show that CXCR3 splice variants have different signaling profiles in response to different ligands, which could lead to different pathophysiological roles. Our data support the concept of biased agonism in CXCR3 variant-mediated signaling and suggest that individual CXCR3 variants might prove to be viable drug targets.

Molecular Pharmacology Fast Forward. Published on August 10, 2016 as DOI: 10.1124/mol.116.105502
This article has not been copyedited and formatted. The final version may differ from this version.

Materials and Methods

Materials. Recombinant chemokines were from PeproTech, Inc. (Rocky Hill, NJ). Coelenterazine 400A for BRET^2 experiments was from Biotium (Hayward, CA). Forskolin, pertussis toxin (PTX) and poly-D-lysine were from Sigma (St. Louis, MO), and the anti-CXCR3 mAb (clone 1C6) directly coupled to phycoerythrin was from R&D Systems (Minneapolis, MN). Dulbecco's modified Eagle's medium Glutamax (DMEM-Q), 1% penicillin-streptomycin and Lipofectamine 2000 were from Life Technologies. BSA fraction V, fatty acid free was from EMD Millipore and 96-well white microplates with clear bottom, and 384-well black microplates with clear bottom plates were from Corning.

Plasmids. The CXCR3A (Uniprot identifier P49682-1) plasmid was purchased from the Missouri S&T cDNA Resource Center (Rolla, MO: www.cdna.org). The cDNA of splice variants CXCR3B (Uniprot identifier P49682-2) and CXCR3Alt (Uniprot identifier P49682-3) were synthesized by Bio Basic (Markham, Canada) and subcloned into pcDNA3.1+ using with *BstE*II and *Xba*I restriction sites. The cAMP EPA2 sensor was a gift from Michel Bouvier (Université de Montréal, Montréal, QC, Canada). CXCR3A-GFP10, CXCR3B-GFP10 and CXCR3Alt-GFP10 were constructed by ligating the coding sequence of CXCR3 isoforms to GFP10, amplified by PCR from the cAMP EPAC reporter using *Xho*I and *Xba*I, or *Not*I and *Xho*I, or *Not*I and *Xba*I, respectively. The amino acid sequence of the linker region between the terminal receptor residue and the fluorophore was described earlier (Berchiche et al., 2011; Percherancier et al., 2005). β-Arrestin1-Rluc3 and β-arrestin2-Rluc3 sensors were constructed by C-terminally fusing the coding sequence of β-arrestin to Rluc3, amplified from the cAMP EPAC reporter

Molecular Pharmacology Fast Forward. Published on August 10, 2016 as DOI: 10.1124/mol.116.105502
This article has not been copyedited and formatted. The final version may differ from this version.

including the linker region, using *Hind*III and *Xba*I unique restriction sites (Leduc et al., 2009). All sequences were verified by direct sequencing.

Cell culture and Transfection. HEK293T cells (passage number 5 to 15, ATCC, Manassas, VA) were maintained in DMEM-Q, 1% penicillin-streptomycin, and 10% fetal bovine serum (Atlanta Biologicals). Transient transfection was performed in six-well plates using the polyethylenimine method as described previously (Percherancier et al., 2005). Transient high-throughput in-plate transfections were performed in 384-well plates using Lipofectamine 2000 according to manufacturer's instructions with some modifications. Briefly, cells were trypsinized, counted and mixed with the DNA-Lipofectamine 2000 complex then directly plated in 0.01% poly-D-lysine coated 384-well plates at a density of 20,000 cells/well. The total amount of transfected DNA was kept constant at 2μg/well for six-well plates and 30ng/well for 384 well plates by adding empty vector pcDNA3.1+. Transfected DNA amounts were adjusted to obtain comparable cell surface expression among the unfused and GFP10- fused CXCR3 splice variants in all experiments.

Flow Cytometry. HEK293T cells transfected in six-well plates with CXCR3 alternative variants were detached in ice cold PBS. Human peripheral blood mononuclear cells (PBMC) obtained by leukapheresis (Gift from Prof. Michel Nussenzweig, The Rockefeller University) and purified T cells (Gift from Dr. Helen Su, NIH/NIAID) obtained using a Pan T cell isolation kit (Miltenyi Biotek), were stimulated with 10 μg/ml phytohemagglutinin (PHA) and cultured for 10 days in RPMI containing 10% fetal bovine serum and 50 IU/ml interleukin-2. Cells were labeled with monoclonal 1C6 phycoerythrin-conjugated antibody (BD Biosciences) that recognizes all three CXCR3

Molecular Pharmacology Fast Forward. Published on August 10, 2016 as DOI: 10.1124/mol.116.105502
This article has not been copyedited and formatted. The final version may differ from this version.

alternative variants for 30 minutes at 4°C in BRET buffer (PBS containing 0.5mM $MgCl_2$ and 0.1% BSA). Cells were then washed three times in ice cold PBS. Cell surface expression was quantified by flow cytometry using the Accuri C6 flow cytometer (BD Biosciences). We also determined receptor surface expression of transfected CXCR3 variants in HEK293T and the total CXCR3 quantities in both activated PBMC and T cells using the Quanti-BRITE standardization beads (BD Biosciences). Receptor quantities typically reached around 1.3 to 2.5 X 10^4 antibody-binding sites per cell for both HEK293T transfected CXCR3 alternative variants and endogenous CXCR3 expressed in activated PBMCs and purified T cells.

BRET Measurements. HEK293T cells transfected in six-well plates were seeded in 0.01% poly-D-Lysine coated 96-well, white microplates with clear bottom 24 hours after transfection at a density of 90,000 cells/well. Forty-eight hours post transfection; media was replaced with BRET buffer. Coelenterazine 400A was added at a final concentration of 5µM followed by a 5 min incubation at room temperature (RT). Luminescence and fluorescence readings were collected using the Synergy NEO plate reader from Biotek (Winooski, USA) and Gen5 software. $BRET^2$ readings between Rluc3 and GFP10 were collected by sequential integration of the signals detected in the 365 to 435 nm (Rluc3) and 505 to 525 nm (GFP10) windows. $BRET^2$ ratios were calculated as described previously (Berchiche et al., 2011; Leduc et al., 2009). All BRET experiments were performed while cells remained attached to the 96-well plates.

Adenylyl cyclase activity. cAMP was determined by using the Rluc3-EPAC-GFP10, a $BRET^2$ cAMP sensor, as described previously (Leduc et al., 2009). Briefly, cells co-transfected with 1.0µg CXCR3A or 1.5µg CXCR3B or 1.0µg CXCR3Alt and 0.03µg

Molecular Pharmacology Fast Forward. Published on August 10, 2016 as DOI: 10.1124/mol.116.105502
This article has not been copyedited and formatted. The final version may differ from this version.

Rluc3-EPAC-GFP10 reporter were seeded into poly-D-lysine coated 96-well plates 24 hours after transfection. Coelenterazine 400A was added to the cells followed by a 5 min incubation at RT. Cells were then stimulated with ligand in the presence of 5μM of forskolin at RT for 3 min. For experiments involving PTX, 100ng/mL of PTX was added to the media and cells were treated with PTX for 16 hours before stimulation with forskolin and chemokines.

Arrestin recruitment. β-Arrestin recruitment was measured by $BRET^2$ by co-transfection of 1.0μg of CXCR3A-GFP10 or 1.5μg of CXCR3B-GFP10 or 0.5μ CXCR3Alt-GFP10 with 0.05μg of β-arrestin2-Rluc3 or β-arrestin1-Rluc3. Transfected cells were seeded into poly-D-lysine coated 96-well plates. We first determined the optimal donor (RLuc3) quantity and then performed acceptor (GFP10) titrations experiments with optimal donor quantity to determine BRETmax ratios of each -GFP10 and -Rluc3 fusion pair as described previously (Berchiche et al., 2007; Bonneterre et al., 2016; Kalatskaya et al., 2009). For dose-response experiments, cells expressing the –GFP10 and –Rluc3 fusion proteins at $BRET^2_{max}$ ratios, were stimulated for 5 min at 37°C with increasing concentrations of the indicated ligand before the addition of the substrate, unless specified otherwise. The values were corrected to net BRET by subtracting the background $BRET^2$ signal detected when the –Rluc3 construct was expressed alone.

Endocytosis. HEK293T transfected with 1.0μg CXCR3A or 1.5μg CXCR3B or 1.0μg CXCR3Alt were incubated with 100nM of chemokines at 37°C with gentle agitation, followed by immediate incubation on ice to stop the reaction. Surface bound chemokines were removed with acid washing (50mM glycine, pH 2.7, 150mM NaCl) and cells subsequently washed twice with ice-cold PBS. Cells were then labeled with anti-CXCR3

Molecular Pharmacology Fast Forward. Published on August 10, 2016 as DOI: 10.1124/mol.116.105502
This article has not been copyedited and formatted. The final version may differ from this version.

1C6 phycoerythrin-conjugated antibody for 30 minutes on ice following manufacturer's instructions. Antibody incubation was followed by two washes with ice-cold PBS. Cell surface receptor expression was quantified by flow cytometry using the Accuri C6 flow cytometer (BD Biosciences). Surface expression of CXCR3 after ligand incubation at 37°C was expressed as percentage of CXCR3 expression compared with a sample drawn before addition of the ligands and kept on ice prior to the acid wash and antibody staining.

Erk1/2 phosphorylation. Chemokine induced MAPK pathway activation was determined by In-Cell Western assay (Li-COR). Briefly, cells were transfected in a high-throughput in-plate transfection manner with 10ng of CXCR3A, 15ng of CXCR3B or 10ng of CXCR3Alt. After 24 hours the media was removed and replaced with 1X Hank's Balanced Salt Solution- 20mM HEPES pH 7.4 supplemented with 0.2 % BSA (HBSS-H 0.2% BSA). Transfected cells were then stimulated with 100nM of chemokines at 37°C for different periods of time (2, 5, 7, 10 and 15 mins) or in the presence of increasing concentration of ligand. ERK activity was stopped by fixing cells with a solution of PBS containing 3.7% formaldehyde for 20 mins at RT. Detection of phosphor-ERK1/2 and total ERK2 proteins were performed as described previously (Wong, 2004). Plates were scanned using the Li-COR Odyssey infrared reader.

Data analysis. Data were analyzed using Prism 6.0 software (GraphPad Software, San Diego, CA). Statistical significance of the differences between the various conditions was determined using one-way analysis of variance with Tukey's post t test or Bonferroni's post t test when appropriate. When indicated, differences of top or bottom values were also determined using sigmoidal dose response simultaneous curve fitting.

Molecular Pharmacology Fast Forward. Published on August 10, 2016 as DOI: 10.1124/mol.116.105502
This article has not been copyedited and formatted. The final version may differ from this version.

Results

Gαi activity of CXCR3 is limited to specific alternative splice variants. We evaluated the ability of CXCR3 alternative splice variants to activate Gαi signaling in response to chemokines (Fig. 1). Receptor cDNA quantities were adjusted to obtain comparable cell surface expression for all CXCR3 variants, which were kept constant across all assays (Supplemental Figure 3). HEK293T cells co-expressing the EPAC cAMP biosensor previously described (Leduc et al., 2009) with CXCR3 alternative variants were stimulated with increasing concentrations of chemokines in the presence of forskolin in live cells and the inhibition of forskolin induced cAMP production as a consequence of Gαi activation was measured.

Chemokine receptor CXCR3A inhibited cAMP production when stimulated with CXCL10 and CXCL11 and both chemokines had similar efficacies and potencies (Fig. 1A, Table 1). These results are in line with previous reports (Scholten et al., 2011). Yet, chemokines CXCL9 and CXCL4 failed to trigger significant Gαi activity even at chemokine concentrations as high as 100nM. Furthermore, CXCR3B mediated Gα activation was only detected after stimulation with 100nM of CXCL11 but not at lower concentrations or in the presence of the other chemokine ligands (Fig. 1B). In addition, we assessed the ability of chemokines to trigger Gαs activation via CXCR3B using the EPAC biosensor in the absence of forskolin (Leduc et al., 2009). As opposed to previously reported Gαs activity in human microvascular endothelial cell line-1 (HMEC-1) stably expressing CXCR3B (Lasagni et al., 2003), we found that in our assays it failed to activate Gαs upon treatment with its chemokine ligands (data not shown). Chemokine receptor variant CXCR3Alt failed to induce significant Gαi activation in response to all

Molecular Pharmacology Fast Forward. Published on August 10, 2016 as DOI: 10.1124/mol.116.105502
This article has not been copyedited and formatted. The final version may differ from this version.

chemokines tested (Fig. 1C), although the truncated receptor was expressed at the cell surface as measured by flow cytometry. Results obtained with CXCR3Alt were similar to our results obtained when cells were co-transfected with the EPAC biosensor and empty vector pcDNA3.1+ (Fig. 1D).

CXCR3 splice variants differentially recruit β-Arrestins. We measured β-arrestin recruitment to CXCR3 in live cells using a BRET proximity assay, which was extensively used to study receptor interaction with arrestins; ligand-induced receptor/arrestin conformational changes as well as receptor dimerization (Berchiche et al., 2011; Hamdan et al., 2005; Kalatskaya et al., 2009). We performed acceptor/donor titration experiments by co-expressing increasing quantities of CXCR3-GFP10 acceptors with fixed quantities of β -arrestin1-Rluc3 or β -arrestin2-Rluc3 donors (Fig. 2). Surprisingly, we measured a significant and saturating basal BRET signal in the absence of ligands for CXCR3A with both β-arrestins and CXCR3B with β -arrestin2, which further increased following stimulation with 100nM CXCL11 (Fig.2A-C). As for CXCR3B/β-arrestin1, acceptor/donor titration in the absence of ligand resulted in a bystander curve, most likely due to random collision of co-expressed BRET pairs (Bonneterre et al., 2016). However, stimulation with CXCL11 resulted in a saturating curve supporting ligand-induced β-arrestin1 recruitment to CXCR3B (Fig. 2D). This suggests a preference of CXCR3B for β-arrestin2 in the absence of ligand. Curve fitting of the data obtained from the titration experiments allowed us to determine both $BRET_{max}$ and $BRET_{50}$ values in the absence and presence of 100nM CXCL11 (Table 2). $BRET_{max}$ corresponds to the best acceptor and donor concentrations determined at saturation with optimal sensitivity, which we used to assess ligand-induced CXCR3/β-arrestin

Molecular Pharmacology Fast Forward. Published on August 10, 2016 as DOI: 10.1124/mol.116.105502
This article has not been copyedited and formatted. The final version may differ from this version.

interaction. Furthermore, $BRET_{50}$ corresponds to the acceptor/donor ratio giving 50% of the maximal signal and reflects the propensity of BRET partners to interact.

Stimulation of CXCR3A/β-arrestin1; CXCR3A/β-arrestin2 as well as CXCR3B/β-arrestin2 pairs with 100nM CXCL11 resulted in an increased $BRET_{max}$ (Fig 2A-C and Table 2) compared to basal conditions. This increase is a direct consequence of changes in the distance and/or orientation between the –Rluc donor and –GFP10 acceptor fusions. This strongly suggests that CXCL11 induces conformational changes in these receptor/β-arrestin preformed complexes. In addition, CXCL11 stimulation also decreased $BRET_{50}$ values shifting the saturation curve to the left for these receptor/arrestin pairs, which indicates a higher propensity of CXCR3A and B variants to interact with β-arrestins in the presence than in the absence of CXCL11 (Table 2).

In contrast, titration of the CXCR3Alt-GFP10 acceptor with both β-arrestins donors showed no ligand-dependent or -independent association indicating that CXCR3Alt does not interact with β-arrestins (Fig. 2E-F).

Moreover, we assessed the specificity of the interactions we measured to ascertain whether select CXCR3 variants interact with β-arrestins in the absence of ligand. We co-transfected cells expressing the $BRET^2$ β-arrestin donor and CXCR3 acceptor fusions with the corresponding FLAG-β-arrestin and measured its impact on the basal BRET signal. We observed a transfected FLAG-β-arrestin quantity-dependent decrease of the basal BRET signal for CXCR3A and both β-arrestins as well as CXCR3B and β-arrestin2, whereas CXCR3B and β-arrestin1 remained unaffected (Fig. 3). A decrease in a dose-dependent manner of the basal BRET signal indicates a competition between the donor fused β-arrestin and the corresponding FLAG-tagged β-arrestin, which in turn

Molecular Pharmacology Fast Forward. Published on August 10, 2016 as DOI: 10.1124/mol.116.105502
This article has not been copyedited and formatted. The final version may differ from this version.

supports a specific ligand-independent interaction between select CXCR3 alternative variants and β-arrestin.

Next, we quantified ligand-mediated β-arrestin recruitment to CXCR3 at $BRET_{max}$ by performing kinetic experiments. These were carried out at RT to fully capture the details of recruitment kinetics following chemokine stimulation (100nM). CXCR3A treatment with CXCL11 or CXCL10 resulted in a rapid β-arrestin2 recruitment reaching a plateau in 5 to 7 mins (Fig 4A). Similar results were obtained with β-arrestin1 (Supplemental Figure 4). A small but statistically significant elevation in β-arrestin2 recruitment to CXCR3A following stimulation with CXCL9 or CXCL4 was also observed (Fig 4A, Supplemental Figure 5). In contrast, CXCL9 or CXCL4 failed to induce β-arrestin1 recruitment to CXCR3A (Supplemental Figure 4A). Our data show that CXCR3A and CXCR3B acceptor fusions are functional and are able to recruit both β-arrestins in response to ligands. In addition, these results indicate a receptor preference for specific β-arrestins, which is selectively influenced by chemokines.

Also, CXCL11 increased β-arrestin2 recruitment to CXCR3B with the signal reaching a plateau within the first 5 mins of stimulation (Fig 4B). CXCL10, CXCL9 and CXCL4, a chemokine suggested to be a selective high affinity ligand of CXCR3B (Lasagni et al., 2003), failed to trigger β-arrestin2 recruitment to CXCR3B. Similar results were obtained with β-arrestin1 (Supplemental Figure 4B). As for CXCR3Alt, all chemokines failed to induce both β-arrestin1 and β-arrestin2 recruitment to this C-terminally truncated alternative variant (Fig. 4C, Supplemental Figure 4C).

To catalog the pharmacology of CXCR3 variants in response to their chemokines, we measured the effect of increasing concentrations of ligands on β-arrestin recruitment to

Molecular Pharmacology Fast Forward. Published on August 10, 2016 as DOI: 10.1124/mol.116.105502
This article has not been copyedited and formatted. The final version may differ from this version.

CXCR3A and CXCR3B (Table 1). Our results obtained with CXCL11 and CXCL10 are consistent with previously reported observations obtained with a BRET1 arrestin proximity assay (Scholten et al., 2011). Indeed, CXCL11 acts as a full agonist with a potency of 8nM, whereas CXCL10 acts as a partial agonist with a potency of 70nM (Fig. 5A) on the β-arrestin2 recruitment to CXCR3A. A similar rank order of potencies was observed with β-arrestin1 (Table 1, Supplemental Figure 6A). As for CXCR3B, CXCL11 caused arrestin recruitment with potencies of 61nM and 33nM for β-arrestin2 and β-arrestin1, respectively (Fig.5B, Table 1, Supplemental Figure 6B). These results suggest that the longer N-terminus of CXCR3B is sufficient to change the receptor's ability to respond to chemokines and recruit β-arrestins. Moreover, these data suggest that although the N-terminal tail of CXCR3Alt is identical to that of CXCR3A, not surprisingly differences in the C-terminus of CXCR3Alt are sufficient to perturb its ability to recruit β-arrestins.

Chemokine triggered β-arrestin recruitment to CXCR3 is PTX insensitive. To determine whether ligand-induced β-arrestin recruitment to CXCR3A and CXCR3B are linked to Gαi signaling, we tested their sensitivity to Gαi/o-inactivating PTX treatment (Fig. 6). Ligand mediated β-Arrestin2 (Fig. 6, A-C) and β-Arrestin1 (Supplemental Figure 7) recruitment to CXCR3A and CXCR3B were resistant to PTX treatment. As expected, PTX treatment inhibited ligand-induced Gαi activity mediated by CXCR3A (Fig.6A). This result suggests that β-arrestin recruitment to CXCR3A occurs independently from Gαi signaling in response to CXCL11 and CXCL10. PTX treatment also impaired CXCL11 triggered CXCR3B Gαi activity even if it was only detected with 100nM of chemokine (Fig.6 C) comparably to CXCR3A.

Molecular Pharmacology Fast Forward. Published on August 10, 2016 as DOI: 10.1124/mol.116.105502
This article has not been copyedited and formatted. The final version may differ from this version.

Chemokines induce internalization of all CXCR3 splice variants. We stimulated HEK293T cells expressing CXCR3 variants with chemokine ligands (100nM) for various time periods at 37°C to assess ligand-induced receptor internalization. Excess chemokine was removed by acid wash and remaining surface receptors were quantified by flow cytometry. Stimulation with chemokines induced internalization of all receptor variants (Fig. 7). Chemokine CXCL11 induced CXCR3A internalization was modest in comparison to the other chemokines tested for this receptor variant, yet our results with CXCL11 remain comparable to previously reported observations (Scholten et al., 2011). Moreover, nearly 40% of CXCR3A receptors internalized within the first 10 mins of stimulation with CXCL10 and CXCL4, compared with CXCL9, which required 30 mins of stimulation to reach 40% internalization. Similarly, nearly 50% of CXCR3B receptors internalized during the first 10 mins after incubation with CXCL10, CXCL9 and CXCL4. Yet CXCL11 only induced moderate receptor internalization in the same fashion as CXCL11-induced CXCR3A internalization. Interestingly, CXCL11, CXCL9 and CXCL4 induced a robust and rapid CXCR3Alt internalization, while CXCL10 had little to no effect. Surprisingly, in our assay CXCL4 (100nM), a CXCR3B ligand, induced robust receptor internalization of all three CXCR3 variants. CXCL4 chemokine is reported to bind to CXCR3A and trigger chemotaxis at high chemokine concentrations of 500 to 750nM (Korniejewska et al., 2011; Mueller et al., 2008). Our results indicate that all ligands (100nM) are able to bind CXCR3 variants expressed at the cell surface and thus trigger their function

CXCR3 splice variants display different ERK1/2 phosphorylation profiles. We quantitatively measured ligand-induced ERK1/2 phosphorylation in HEK293T cells

Molecular Pharmacology Fast Forward. Published on August 10, 2016 as DOI: 10.1124/mol.116.105502
This article has not been copyedited and formatted. The final version may differ from this version.

expressing CXCR3 variants. Transfected cells were stimulated with chemokines (100nM) at 37°C for various time periods (Fig. 8A,C-D). ERK1/2 phosphorylation was quantified using an InCell Western approach. This method was previously used to measure ERK1/2 phosphorylation of cannabinoid receptor CB1, a member of the GPCR family coupled to Gαi/o heterotrimeric G proteins (Daigle et al., 2008). Three out of the four chemokines tested induced CXCR3A mediated ERK1/2 phosphorylation (Fig. 8A). In cells expressing CXCR3A, CXCL11 induced the longest and most significant response starting as early as 2 mins following ligand addition (294 ± 37% of basal) and lasting 10 mins (247 ± 21% of basal) with a peak phosphorylation measured at 5 mins (402 ± 37% of basal). In comparison to CXCL11, CXCL10-mediated ERK1/2 phosphorylation through CXCR3A was shorter and more modest. Its signal was detected between 2 mins (250 ± 60% of basal) and 5 mins (199 ± 25% of basal) following stimulation. Chemokine CXCL9 also triggered a moderate elevation of ERK1/2 phosphorylation starting at 5 mins (225 ± 24% of basal), which declined after 10 mins (217 ± 26% of basal). In contrast, CXCR3B activation by chemokines showed a different ERK1/2 phosphorylation profile than for CXCR3A (Fig. 8B). Indeed, CXCL11 triggered a modest ERK1/2 phosphorylation starting at 5 mins (203 ± 18% of basal) and lasted 10 mins (170 ± 13% of basal). Moreover, CXCL9 also induced a short ERK1/2 phosphorylation, peaking at 10 mins (192 ± 22 % of basal) and a short and weak, yet statistically significant, signal at 5 mins (159 ± 22 % of basal) following stimulation with CXCL4. Surprisingly, cells expressing CXCR3Alt variant also responded to ligands and we measured ERK1/2 phosphorylation following stimulation with CXCL11, CXCL10 and CXCL9 (Fig. 8D). Treatment with CXCL11 increased ERK1/2 phosphorylation between 5 to 10 mins, with

Molecular Pharmacology Fast Forward. Published on August 10, 2016 as DOI: 10.1124/mol.116.105502
This article has not been copyedited and formatted. The final version may differ from this version.

a peak phosphorylation detected after 7 mins (195 ± 16 % of basal). We also quantified, modest but extended from 5 to 15 mins of ERK1/2 phosphorylation following treatment with CXCL10. In contrast, CXCL9 triggered ERK1/2 phosphorylation at a single time point of 10 mins (155 ± 14 % of basal).

Compared to CXCR3A, chemokines induced weaker ERK1/2 phosphorylation through CXCR3B and CXCR3Alt. However, these changes were statistically significant when compared to cells transfected with the receptor and treated with assay buffer only. Furthermore, to ensure that the signals were indeed the result of CXCR3 alternative variants, all experiments were performed in parallel with cells transfected with empty vector pcDNA3.1+. These cells failed to respond to chemokines (data not shown), indicating that the responses measured for CXCR3 were ligand-induced and receptor-variant specific. We also collected pharmacological data for CXCR3A by taking advantage of favorable dynamic range and the quantitative nature of the ERK1/2 phosphorylation In-Cell Western assay. We measured ERK1/2 phosphorylation in cells transfected with CXCR3A in response to increasing concentrations of CXCL11 and CXCL10 (Fig. 8B). Our results indicate that both CXCL11 and CXCL10 induce ERK1/2 phosphorylation with similar efficacy and potency and are full agonists for this pathway (Table 1).

Molecular Pharmacology Fast Forward. Published on August 10, 2016 as DOI: 10.1124/mol.116.105502
This article has not been copyedited and formatted. The final version may differ from this version.

Discussion

The goal of this study was to explore the specific intracellular signaling pathways activated by CXCR3 splice variants in response to their chemokine ligands. We report that different CXCR3 splice variants induce quantitatively distinctive signaling responses following ligand stimulation and that receptor signaling efficacy depends on the splice variant/chemokine pair assessed. Receptor variant/chemokine pairs and the corresponding pathways activated are summarized in Table 3. The ability of ligands to activate different intracellular signaling pathways via the same receptor to different extents is a widely observed phenomenon and has been documented for many GPCRs, including chemokine receptors. This characteristic has been given several names including biased agonism, stimulus trafficking and functional selectivity. Biased agonism of GPCRs supports the existence of multiple active receptor conformations that ligands may differentially stabilize, leading to the activation of specific signaling pathways (Kenakin, 2007; Kenakin, 2009). The non-redundant signaling responses we report for CXCR3 alternative splice variants could be explained if chemokines stabilized distinct receptor splice variant conformations leading to the activation of different intracellular signaling pathways.

Indeed, CXCR3A-mediated Gαi activity was only detectable in response to CXCL11 and CXCL10, which are in line with the Gαi activity previously reported for this canonical receptor (Scholten et al., 2011). Interestingly, CXCL11 also induced CXCR3B-mediated Gαi activity, yet only at a saturating concentration of 100nM. Sulfation of Tyr27 and Tyr29 in the N-terminal region of CXCR3A is essential for chemokine binding and thus receptor function (Colvin et al., 2006). The longer N-

Molecular Pharmacology Fast Forward. Published on August 10, 2016 as DOI: 10.1124/mol.116.105502
This article has not been copyedited and formatted. The final version may differ from this version.

terminus of CXCR3B contains two additional potential sulfation sites (Tyr6 and Tyr40). These could also be sulfated or influence the sulfation of the Tyr residues common to both variants, and therefore co-translational Tyr sulfation might explain the □α□ activity measured for CXCR3B.

As expected, Gαi activation of CXCR3A was inhibited by PTX treatment. Surprisingly, CXCR3B-induced Gαi activation was also inhibited by PTX treatment suggesting that this Gαi activity is specific. Relatedly, stimulation of CXCR3A with CXCL11 or CXCR10 and of CXCR3B with CXCL11 further increased basal β-arrestin recruitment to the receptor and was PTX insensitive. Taken together, our results indicate that ligand mediated Gα□ signaling and β-arrestin recruitment occur independently from each other. Our findings also suggest that chemokine receptor variant/ligand pairs selectively determine the receptor/β-arrestin conformation as well as the efficacy of Gαi activity. Similarly to the ligand initiated β-arrestin recruitment and Gαi signaling, we report that the CXCR3-mediated ERK1/2 phosphorylation intensity and signal duration measured depend on the splice variant /chemokine pair assessed. For example, CXCL11-mediated ERK1/2 phosphorylation through CXCR3A was stronger and lasted longer than the one mediated through both CXCR3B and CXCR3Alt.

Ligand-independent β-arrestin recruitment was previously reported for chemokine receptor CCR1 (Gilliland et al., 2013), atypical chemokine receptor ACKR2/D6 (McCulloch et al., 2008) as well as a chimeric receptor composed of ACKR3/CXCR7 with its C-terminal tail swapped with CXCR4 (Gravel et al., 2010). C-terminal tails of both D6 and CCR1 show basal phosphorylation, which plays an important role in their ligand independent activity. Our data are the first to indicate that ligand independent β-

Molecular Pharmacology Fast Forward. Published on August 10, 2016 as DOI: 10.1124/mol.116.105502
This article has not been copyedited and formatted. The final version may differ from this version.

arrestin recruitment can also differentially occur for the different CXCR3 alternative splice variants. Such constitutive β-arrestin recruitment to CXCR3A and CXCR3B might also arise from low levels of basal receptor phosphorylation. Indeed, the C-terminal tail of CXCR3A and CXCR3B contains nine Ser residues and one Thr residue that might allow for some basal level of Ser/Thr phosphorylation, favoring the interaction with β-arrestins. An earlier report of a low level of phosphorylation measured for transfected CXCR3 further supports this hypothesis (Colvin et al., 2004).

Receptor internalization may occur in both β-arrestin-dependent and -independent fashion. Here, we demonstrate that the internalization profiles of all three CXCR3 alternative splice variants fail to correlate with ligand-induced β-arrestin recruitment, supporting a β-arrestin-independent internalization mechanism. Similarly, Rajagopal et al. recently showed that CXCL11-induced β-arrestin recruitment to the canonical CXCR3 receptor does not correlate with CXCL11-induced internalization (Rajagopal et al., 2013). Likewise, CXCL11 and CXCL10 provoked receptor internalization in a β-arrestin independent fashion when CXCR3A was expressed in L1.2 murine cells (Meiser et al., 2008). Furthermore, β-arrestins are well recognized for their role as scaffold proteins for downstream signaling phosphorylation cascades (DeWire et al., 2007). ERK1/2 phosphorylation induced by CXCR3 splice variants does not correlate either with ligand induced β-arrestin recruitment. This indicates that β-arrestin may not be required for ERK1/2 phosphorylation provoked by specific receptor variant/ligand pairs such as CXCR3B/CXCL9 and CXCR3Alt/CXCL10. Nevertheless, β-arrestins may play a role in ERK1/2 phosphorylation provoked by the CXCR3A/CXCL11 pair. Similarly, only CXCR3A/CXCL11 and CXCR3A/CXCL10 pairs provoke Gαi activity that correlates

Molecular Pharmacology Fast Forward. Published on August 10, 2016 as DOI: 10.1124/mol.116.105502
This article has not been copyedited and formatted. The final version may differ from this version.

with their ERK1/2 phosphorylation profile, supporting the possibility that ERK1/2 phosphorylation may be a consequence of Gαi activation.

Many GPCRs with highly truncated alternative splice variants lacking some TM helices are reported in the literature (Wise, 2012). Alternative splice variant CXCR3Alt is a predicted five TM domain receptor with a short C-terminal end (Ehlert et al., 2004). CXCR3Alt lacks the third intracellular loop important for G protein interaction and subsequent activation of intracellular components (Thelen and Thelen, 2008). Stimulation of this splice variant resulted in weak but statistically significant ERK1/2 phosphorylation and chemokine-induced receptor internalization. Nevertheless, CXCR3Alt failed to induce Gαi activation and β-arrestin recruitment in the absence or presence of chemokines. Compared with CXCR3A and CXCR3B, the C-terminus of CXCR3Alt lacks the Ser and Thr phosphorylation sites typically phosphorylated by GRKs and required for β-arrestin recruitment. This fundamental difference of CXCR3Alt and its limited signaling further supports the idea that CXCR3 splice variants play different roles in fine tuning chemokine induced signaling responses.

It may be speculated that CXCR3Alt splice variant behaves as an atypical chemokine receptor. Its role could be to scavenge chemokines and contribute to the establishment of a chemokine gradient, similarly to chemokine receptor CXCR7, which does not activate Gαi heterotrimeric G protein, yet still recruits β-arrestin and induces ERK1/2 phosphorylation and internalization in response to CXCL12 (Boldajipour et al., 2008; Kalatskaya et al., 2009; Levoye et al., 2009). Another explanation for our results could be that the role of CXCR3Alt is to modulate the function of a chemokine receptor such as CXCR3A since these variants can be co-expressed in cells (Aksoy et al., 2006)

Molecular Pharmacology Fast Forward. Published on August 10, 2016 as DOI: 10.1124/mol.116.105502
This article has not been copyedited and formatted. The final version may differ from this version.

and since truncated GPCRs could act as dominant negative of CXCR3A (Wise, 2012). The later possibility is further supported by the atypical and predicted five TM arrangement of CXCR3Alt. An additional possibility could be that activation of CXCR3Alt leads to other functional consequences we did not assess. For example, coupling to $G\alpha_{12/13}$ (Kouroumalis et al., 2005) or Gαi proteins isoforms i2 and i3 (Thompson et al., 2007) are also reported for CXCR3.

We cannot rule out that our observations are cell-type specific, yet CXCR3 natural ligands behave as perfect biased ligands (Kenakin and Christopoulos, 2013), which activate only specific signaling pathways but not others. For example, CXCL4 induces internalization of all variants, modestly stimulates ERK1/2 phosphorylation via CXCR3B and yet has no other effects on any of the receptor variants in the pathways assessed. Lack of signaling in our assays of specific CXCR3 variant/chemokine pairs could also be explained by the need of a GPCR modifying protein such as CXCR3A splice variant to induce signaling, which in turn could contribute to further diversify CXCR3-mediated signaling. Another possibility is that specific CXCR3 alternative splice variants that do not signal in our assays play a role to internalize specific chemokines and help establish gradients in specific tissues.

Nevertheless, the differences we report support that CXCR3 ligands stabilize different conformations of CXCR3 splice variants. As a consequence, each CXCR3 variant/chemokine pair is likely to fulfill different functions *in vivo*. Although other chemokines receptors, such as CCR2 and (Charo et al., 1994), CCR9 (Yu et al., 2000), possess alternative splice variants with some differences expression and signaling levels (Sanders et al., 2000; Wong et al., 1997), our work is the first to quantify the function of

chemokine receptor CXCR3 alternative splice variants in response to its four natural ligands across multiple four signaling pathways.

In addition, our work provides insight into the differences in the signaling abilities of CXCR3 alternative splice variants that are a direct consequence of their differences in the N- and C-terminal regions and intracellular loops. Our finding that chemokine receptor CXCR3 splice variants are able to selectively stimulate specific signaling pathways in response to different chemokines supports the idea that the chemokine system is not functionally redundant. Instead, the different activation patterns of CXCR3 splice variants indicate that the chemokine system displays an additional layer of complexity fine tuned by receptor splice variants. The differences in CXCR3 variant/chemokine pair signaling must be taken into account in the context of targeting CXCR3 with small molecules. Furthermore, these differences could form a basis to design small molecules that selectively modulate in a biased manner specific receptor alternative splice variants in disease settings.

Molecular Pharmacology Fast Forward. Published on August 10, 2016 as DOI: 10.1124/mol.116.105502
This article has not been copyedited and formatted. The final version may differ from this version.

Acknowledgments

We thank the Bouvier lab for the gift of the EPAC cAMP reporter. We thank Prof. Michel Nussenzweig for the gift of Human peripheral blood mononuclear cells (PBMC) as well as Dr. Helen Su for the gift of purified Human T cells. We also thank Dr. Cassandra Koole and Dr. Alexandre Fürstenberg for critical reading of the manuscript and Manija Kazmi as well as the other members of the Sakmar laboratory.

Authorship contributions

Participated in research design: Berchiche, Sakmar

Conducted experiments: Berchiche

Performed data analysis: Berchiche

Wrote manuscript: Berchiche and Sakmar**.**

References

Aksoy MO, Yang Y, Ji R, Reddy PJ, Shahabuddin S, Litvin J, Rogers TJ and Kelsen SG (2006) CXCR3 surface expression in human airway epithelial cells: cell cycle dependence and effect on cell proliferation. *American journal of physiology Lung cellular and molecular physiology* **290**:L909-918.

Berchiche YA, Chow KY, Lagane B, Leduc M, Percherancier Y, Fujii N, Tamamura H, Bachelerie F and Heveker N (2007) Direct assessment of CXCR4 mutant conformations reveals complex link between receptor structure and G(alpha)(i) activation. *The Journal of biological chemistry* **282**:5111-5115.

Berchiche YA, Gravel S, Pelletier ME, St-Onge G and Heveker N (2011) Different effects of the different natural CC chemokine receptor 2b ligands on beta-arrestin recruitment, Galphai signaling, and receptor internalization. *Molecular pharmacology* **79**:488-498.

Boldajipour B, Mahabaleshwar H, Kardash E, Reichman-Fried M, Blaser H, Minina S, Wilson D, Xu Q and Raz E (2008) Control of chemokine-guided cell migration by ligand sequestration. *Cell* **132**:463-473.

Bonneterre J, Montpas N, Boularan C, Gales C and Heveker N (2016) Analysis of Arrestin Recruitment to Chemokine Receptors by Bioluminescence Resonance Energy Transfer. *Methods in enzymology* **570**:131-153.

Brady AE and Limbird LE (2002) G protein-coupled receptor interacting proteins: emerging roles in localization and signal transduction. *Cellular signalling* **14**:297-309.

Charo IF, Myers SJ, Herman A, Franci C, Connolly AJ and Coughlin SR (1994) Molecular cloning and functional expression of two monocyte chemoattractant protein 1 receptors reveals alternative splicing of the carboxyl-terminal tails. *Proceedings of the National Academy of Sciences of the United States of America* **91**:2752-2756.

Cole KE, Strick CA, Paradis TJ, Ogborne KT, Loetscher M, Gladue RP, Lin W, Boyd JG, Moser B, Wood DE, Sahagan BG and Neote K (1998) Interferon-inducible T cell alpha chemoattractant (I-TAC): a novel non-ELR CXC chemokine with potent activity on activated T cells through selective high affinity binding to CXCR3. *The Journal of experimental medicine* **187**:2009-2021.

Colvin RA, Campanella GS, Manice LA and Luster AD (2006) CXCR3 requires tyrosine sulfation for ligand binding and a second extracellular loop arginine residue for ligand-induced chemotaxis. *Molecular and cellular biology* **26**:5838-5849.

Colvin RA, Campanella GS, Sun J and Luster AD (2004) Intracellular domains of CXCR3 that mediate CXCL9, CXCL10, and CXCL11 function. *The Journal of biological chemistry* **279**:30219-30227.

Daigle TL, Kearn CS and Mackie K (2008) Rapid CB1 cannabinoid receptor desensitization defines the time course of ERK1/2 MAP kinase signaling. *Neuropharmacology* **54**:36-44.

DeWire SM, Ahn S, Lefkowitz RJ and Shenoy SK (2007) β-Arrestins and Cell Signaling. *Annual Review of Physiology* **69**:483-510.

Ehlert JE, Addison CA, Burdick MD, Kunkel SL and Strieter RM (2004) Identification and partial characterization of a variant of human CXCR3 generated by posttranscriptional exon skipping. *J Immunol* **173**:6234-6240.

Garcia-Lopez MA, Sanchez-Madrid F, Rodriguez-Frade JM, Mellado M, Acevedo A, Garcia MI, Albar JP, Martinez C and Marazuela M (2001) CXCR3 chemokine receptor distribution in normal and inflamed tissues: expression on activated lymphocytes, endothelial cells, and dendritic cells. *Laboratory investigation; a journal of technical methods and pathology* **81**:409-418.

Gilliland CT, Salanga CL, Kawamura T, Trejo J and Handel TM (2013) The chemokine receptor CCR1 is constitutively active, which leads to G protein-independent, beta-arrestin-mediated internalization. *The Journal of biological chemistry* **288**:32194-32210.

Gravel S, Malouf C, Boulais PE, Berchiche YA, Oishi S, Fujii N, Leduc R, Sinnett D and Heveker N (2010) The peptidomimetic CXCR4 antagonist TC14012 recruits beta-arrestin to CXCR7: roles of receptor domains. *The Journal of biological chemistry* **285**:37939-37943.

Groom JR and Luster AD (2011a) CXCR3 in T cell function. *Experimental cell research* **317**:620-631.

Groom JR and Luster AD (2011b) CXCR3 ligands: redundant, collaborative and antagonistic functions. *Immunology and cell biology* **89**:207-215.

Hamdan FF, Audet M, Garneau P, Pelletier J and Bouvier M (2005) High-throughput screening of G protein-coupled receptor antagonists using a bioluminescence

resonance energy transfer 1-based beta-arrestin2 recruitment assay. *J Biomol Screen* **10**:463-475.

Hancock WW, Lu B, Gao W, Csizmadia V, Faia K, King JA, Smiley ST, Ling M, Gerard NP and Gerard C (2000) Requirement of the chemokine receptor CXCR3 for acute allograft rejection. *The Journal of experimental medicine* **192**:1515-1520.

Kalatskaya I, Berchiche YA, Gravel S, Limberg BJ, Rosenbaum JS and Heveker N (2009) AMD3100 is a CXCR7 ligand with allosteric agonist properties. *Molecular pharmacology* **75**:1240-1247.

Kenakin T (2007) Collateral efficacy in drug discovery: taking advantage of the good (allosteric) nature of 7TM receptors. *Trends in pharmacological sciences* **28**:407-415.

Kenakin T (2009) Functional Selectivity: Theoretical Considerations and Future Directions.9-24.

Kenakin T and Christopoulos A (2013) Signalling bias in new drug discovery: detection, quantification and therapeutic impact. *Nature reviews Drug discovery* **12**:205-216.

Korniejewska A, McKnight AJ, Johnson Z, Watson ML and Ward SG (2011) Expression and agonist responsiveness of CXCR3 variants in human T lymphocytes. *Immunology* **132**:503-515.

Kouroumalis A, Nibbs RJ, Aptel H, Wright KL, Kolios G and Ward SG (2005) The chemokines CXCL9, CXCL10, and CXCL11 differentially stimulate G alpha i-

independent signaling and actin responses in human intestinal myofibroblasts. *J Immunol* **175**:5403-5411.

Lasagni L, Francalanci M, Annunziato F, Lazzeri E, Giannini S, Cosmi L, Sagrinati C, Mazzinghi B, Orlando C, Maggi E, Marra F, Romagnani S, Serio M and Romagnani P (2003) An alternatively spliced variant of CXCR3 mediates the inhibition of endothelial cell growth induced by IP-10, Mig, and I-TAC, and acts as functional receptor for platelet factor 4. *The Journal of experimental medicine* **197**:1537-1549.

Leduc M, Breton B, Gales C, Le Gouill C, Bouvier M, Chemtob S and Heveker N (2009) Functional selectivity of natural and synthetic prostaglandin EP4 receptor ligands. *The Journal of pharmacology and experimental therapeutics* **331**:297-307.

Levoye A, Balabanian K, Baleux F, Bachelerie F and Lagane B (2009) CXCR7 heterodimerizes with CXCR4 and regulates CXCL12-mediated G protein signaling. *Blood* **113**:6085-6093.

Li K, Zhu Z, Luo J, Fang J, Zhou H, Hu M, Maskey N and Yang G (2015) Impact of chemokine receptor CXCR3 on tumor-infiltrating lymphocyte recruitment associated with favorable prognosis in advanced gastric cancer. *Int J Clin Exp Pathol* **8**:14725-14732.

Lleo A, Zhang W, Zhao M, Tan Y, Bernuzzi F, Zhu B, Liu Q, Tan Q, Malinverno F, Valenti L, Jiang T, Tan L, Liao W, Coppel R, Invernizzi P, Lu Q, Adams DH, Gershwin ME and Group PBCES (2015) DNA methylation profiling of the X

chromosome reveals an aberrant demethylation on CXCR3 promoter in primary biliary cirrhosis. *Clin Epigenetics* **7**:61.

Loetscher M, Gerber B, Loetscher P, Jones SA, Piali L, Clark-Lewis I, Baggiolini M and Moser B (1996) Chemokine receptor specific for IP10 and mig: structure, function, and expression in activated T-lymphocytes. *The Journal of experimental medicine* **184**:963-969.

Ludeman JP and Stone MJ (2014) The structural role of receptor tyrosine sulfation in chemokine recognition. *British journal of pharmacology* **171**:1167-1179.

Manousou P, Kolios G, Drygiannakis I, Pyrovolaki K, Bourikas L, Papadaki HA and Kouroumalis E (2008) Expression of a splice variant of CXCR3 in Crohn's disease patients; indication for a lymphocyte--epithelial cell interaction. *Journal of gastroenterology and hepatology* **23**:1823-1833.

McCulloch CV, Morrow V, Milasta S, Comerford I, Milligan G, Graham GJ, Isaacs NW and Nibbs RJ (2008) Multiple roles for the C-terminal tail of the chemokine scavenger D6. *The Journal of biological chemistry* **283**:7972-7982.

Meiser A, Mueller A, Wise EL, McDonagh EM, Petit SJ, Saran N, Clark PC, Williams TJ and Pease JE (2008) The chemokine receptor CXCR3 is degraded following internalization and is replenished at the cell surface by de novo synthesis of receptor. *J Immunol* **180**:6713-6724.

Mueller A, Meiser A, McDonagh EM, Fox JM, Petit SJ, Xanthou G, Williams TJ and Pease JE (2008) CXCL4-induced migration of activated T lymphocytes is mediated by the chemokine receptor CXCR3. *Journal of leukocyte biology* **83**:875-882.

Murphy PM, Baggiolini M, Charo IF, Hebert CA, Horuk R, Matsushima K, Miller LH, Oppenheim JJ and Power CA (2000) International union of pharmacology. XXII. Nomenclature for chemokine receptors. *Pharmacological reviews* **52**:145-176.

Percherancier Y, Berchiche YA, Slight I, Volkmer-Engert R, Tamamura H, Fujii N, Bouvier M and Heveker N (2005) Bioluminescence resonance energy transfer reveals ligand-induced conformational changes in CXCR4 homo- and heterodimers. *The Journal of biological chemistry* **280**:9895-9903.

Proudfoot AE, Handel TM, Johnson Z, Lau EK, LiWang P, Clark-Lewis I, Borlat F, Wells TN and Kosco-Vilbois MH (2003) Glycosaminoglycan binding and oligomerization are essential for the in vivo activity of certain chemokines. *Proceedings of the National Academy of Sciences of the United States of America* **100**:1885-1890.

Rajagopal S, Bassoni DL, Campbell JJ, Gerard NP, Gerard C and Wehrman TS (2013) Biased agonism as a mechanism for differential signaling by chemokine receptors. *The Journal of biological chemistry* **288**:35039-35048.

Sanders SK, Crean SM, Boxer PA, Kellner D, LaRosa GJ and Hunt SW, 3rd (2000) Functional differences between monocyte chemotactic protein-1 receptor A and monocyte chemotactic protein-1 receptor B expressed in a Jurkat T cell. *J Immunol* **165**:4877-4883.

Schall TJ and Proudfoot AE (2011) Overcoming hurdles in developing successful drugs targeting chemokine receptors. *Nature reviews Immunology* **11**:355-363.

Scholten DJ, Canals M, Wijtmans M, de Munnik S, Nguyen P, Verzijl D, de Esch IJ, Vischer HF, Smit MJ and Leurs R (2011) Pharmacological characterization of a small-molecule agonist for the chemokine receptor CXCR3. *British journal of pharmacology* **166**:898-911.

Smit MJ, Verdijk P, van der Raaij-Helmer EM, Navis M, Hensbergen PJ, Leurs R and Tensen CP (2003) CXCR3-mediated chemotaxis of human T cells is regulated by a Gi- and phospholipase C-dependent pathway and not via activation of MEK/p44/p42 MAPK nor Akt/PI-3 kinase. *Blood* **102**:1959-1965.

Thelen M and Thelen S (2008) CXCR7, CXCR4 and CXCL12: an eccentric trio? *Journal of neuroimmunology* **198**:9-13.

Thompson BD, Jin Y, Wu KH, Colvin RA, Luster AD, Birnbaumer L and Wu MX (2007) Inhibition of G alpha i2 activation by G alpha i3 in CXCR3-mediated signaling. *The Journal of biological chemistry* **282**:9547-9555.

Wise H (2012) The roles played by highly truncated splice variants of G protein-coupled receptors. *Journal of molecular signaling* **7**:13.

Wong LM, Myers SJ, Tsou CL, Gosling J, Arai H and Charo IF (1997) Organization and differential expression of the human monocyte chemoattractant protein 1 receptor gene. Evidence for the role of the carboxyl-terminal tail in receptor trafficking. *The Journal of biological chemistry* **272**:1038-1045.

Wong SK (2004) A 384-well cell-based phospho-ERK assay for dopamine D2 and D3 receptors. *Analytical biochemistry* **333**:265-272.

Wu Q, Dhir R and Wells A (2012) Altered CXCR3 isoform expression regulates prostate cancer cell migration and invasion. *Molecular cancer* **11**:3.

Yu CR, Peden KW, Zaitseva MB, Golding H and Farber JM (2000) CCR9A and CCR9B: two receptors for the chemokine CCL25/TECK/Ck beta-15 that differ in their sensitivities to ligand. *J Immunol* **164**:1293-1305.

Zhu G, Yan HH, Pang Y, Jian J, Achyut BR, Liang X, Weiss JM, Wiltrout RH, Hollander MC and Yang L (2015) CXCR3 as a molecular target in breast cancer metastasis: inhibition of tumor cell migration and promotion of host anti-tumor immunity. *Oncotarget* **6**:43408-43419.

Zweemer AJ, Toraskar J, Heitman LH and AP IJ (2014) Bias in chemokine receptor signalling. *Trends in immunology* **35**:243-252.

Footnotes

Yamina A. Berchiche was supported by a Fonds de la Recherche en Santé du Québec fellowship, Québec, Canada.

Yamina A. Berchiche's current affiliation: B cell Molecular Immunology Section, Laboratory of Immunoregulation, National Institute of Allergy and Infectious Diseases, US National Institutes of Health, Bethesda, Maryland, USA.

Molecular Pharmacology Fast Forward. Published on August 10, 2016 as DOI: 10.1124/mol.116.105502
This article has not been copyedited and formatted. The final version may differ from this version.

Legends for Figures

Fig 1. CXCR3 alternative splice variants display different Gαi activities in response to their chemokines. Receptor splice variants A, CXCR3A, B, CXCR3B C, CXCR3Alt or D, empty vector pcDNA3.1+ were co-transfected with the cAMP Rluc3-EPAC-GFP10 sensor in HEK293T cells. Cells were exposed to 5μM forskolin with increasing concentrations of the indicated ligands at room temperature for five minutes prior to readings. Results are expressed as the % of inhibition of forskolin-induced cAMP production. Data are reported as mean values of four to six independent experiments performed in triplicate ± S.E.M.

Fig 2. CXCR3A variants constitutively interact with select β-arrestins. Acceptor /donor titration curves of CXCR3 splice variants fused with GFP10 and β-arrestin-Rluc3 were obtained following transfection of HEK293T cells with increasing quantities of CXCR3-GFP10 fusion with 0.05μg β-arrestin-Rluc3 fusions as indicated. Measurements were carried out at room temperature in the absence or presence of 100nM CXCL11. Data were plotted and fitted to a one-site binding hyperbola equation. $BRET_{50}$ and $BRET_{max}$ values were calculated for each $BRET^2$ couple. Results obtained from at least three independent experiments, carried out in triplicate ± S.E.M are shown.

Fig 3. Constitutive β-arrestin interaction is receptor variant specific. HEK293T cells transfected with the indicated receptor variant/β-arrestin at $BRET_{max}$, in the absence (control) or presence of increasing levels of C-terminallyFLAG-□□□□□□ β-arrestin.

Molecular Pharmacology Fast Forward. Published on August 10, 2016 as DOI: 10.1124/mol.116.105502
This article has not been copyedited and formatted. The final version may differ from this version.

The fold increase shown on the x axis represents the ratio of micrograms of β-arrestin-Rluc3 to β-arrestin-FLAG transfected in cells co-expressing CXCR3 variant GFP10 fusion. Statistical significance of the differences between the control, in the absence of FLAG-□□□□□□ β-arrestin, and increasing levels of co-expressed C-terminallyFLAG-□□□□□□ β-arrestin: *, p< 0.05, **, p< 0.01, ***, p< 0.001, ****, p< 0.0001 (One-way ANOVA, Bonferroni's multiple comparison test). Results obtained for three independent experiments carried out in triplicate ± S.E.M are shown.

Fig 4. Receptor variants selectively recruit β-arrestin2 in response to 100nM of chemokines. HEK293T cells transiently co-expressing the indicated CXCR3 variant GFP10 fusion with β-arrestin2-Rluc3 at $BRET_{max}$ were incubated with 100nM of the indicated ligands at room temperature. BRET was measured immediately following ligand addition. Data are reported as mean values of four independent experiments performed in duplicate ± S.E.M.

Fig 5. CXCR3A and CXCR3B recruit β-arrestin2 in the presence of increasing concentrations of chemokine. HEK293T cells transiently co-expressing CXCR3A-GFP10 or CXCR3B-GFP10 with β-arrestin2-Rluc3 at $BRET_{max}$ were incubated with increasing concentrations of the indicated ligands for 5 minutes at 37°C. BRET was measured five minutes following ligand addition. Data are reported as the mean values of three independent experiments performed in triplicate ± S.E.M (see Table 1 for curve fitting parameters).

Fig 6. PTX treatment only affects chemokine induced Gαi activity of CXCR3A and CXCR3B. HEK293T cells transfected with CXCR3 and the EPAC cAMP biosensor or CXCR3-GFP10 fusion with β-arrestin2-Rluc3 were incubated with 100ng/ml PTX for 16 hours at 37°C. Gαi activity of A, CXCR3A and C, CXCR3B are expressed as the % of forskolin-induced cAMP production in the presence of 100nM of the indicated chemokine in the absence or presence of PTX. The forskolin induced cAMP production measured in the absence of chemokine and PTX was set to 100% (white bars). β-arrestin2 recruitment to B, CXCR3A and D, CXCR3B induced with 100nM of the indicated ligands in the absence or presence of PTX. Results represent data obtained from three to five independent experiments performed in triplicate ± S.E.M.

Fig 7. Chemokines induce CXCR3 splice variant's internalization. HEK293T cells expressing CXCR3A; CXCRB and CXCR3Alt were incubated with 100nM of each chemokine at 37°C. Aliquots were removed on ice at the indicated times following ligand addition. Surface-bound ligand was removed by acid washing, and remaining surface CXCR3 was measured by flow cytometry. Data are mean of three to four independent experiments ± S.E.M.

Fig 8. CXCR3 variants induced ERK1/2 phosphorylation with different intensities following stimulation with chemokines. HEK293T cells transiently expressing CXCR3 variants were incubated at 37°C with the indicated ligands, A, CXCR3A, C, CXCR3B D, CXCR3Alt with 100nM of chemokines at the indicated times or B, CXCR3A with increasing concentrations of CXCL11 and CXCL10 at maximum stimulation time of 5 and 2 minutes, respectively. Data are reported as mean values of at least four independent

Molecular Pharmacology Fast Forward. Published on August 10, 2016 as DOI: 10.1124/mol.116.105502
This article has not been copyedited and formatted. The final version may differ from this version.

experiments performed in duplicate ± S.E.M. Statistical significance of the differences between stimulated and control condition: *, $p< 0.05$, **, $p< 0.01$, ***, $p< 0.001$, ****, $p< 0.0001$ (One-way ANOVA, Bonferroni's multiple comparison test).

Molecular Pharmacology Fast Forward. Published on August 10, 2016 as DOI: 10.1124/mol.116.105502
This article has not been copyedited and formatted. The final version may differ from this version.

Table 1. Summary of fitted curve parameters for results shown in Figs. 1 (Gαi activity), 5 (β-arrestin recruitment) and 8 (ERK1/2 phosphorylation). pEC_{50} values are given and maximal responses are shown in absolute (β-arrestin recruitment) and relative (ERK1/2 phosphorylation and Gαi activity) units. Errors are presented as ± S.E.M.

Molecular Pharmacology Fast Forward. Published on August 10, 2016 as DOI: 10.1124/mol.116.105502
This article has not been copyedited and formatted. The final version may differ from this version.

Table 1 (continued)

	CXCR3A		CXCR3B
	CXCL11	CXCL10	CXCL11
cAMP inhibition			
N	4	4	6
IC_{50} (nM)	0.7	0.5	ND
pIC_{50} ± S.E.M.	-9.5 ± 0.3	-9.4 ± 0.2	ND
E_{max} ± S.E.M.	89 ± 11	70 ± 7	ND
β-arrestin2			
N	3	3	3
EC_{50} (nM)	8	71	61
pEC_{50} ± S.E.M.	-8.2 ± 0.1	-7.3 ± 0.2	-7.2 ± 0.1
$BRET^2_{max}$ ± S.E.M.	0.11 ± 0.01	0.07 ± 0.01	0.026 ±0.001 α
β-arrestin1			
N	3	3	3
EC_{50} (nM)	16	32	33
pEC_{50} ± S.E.M.	-7.8 ± 0.1	-7.5 ± 0.1	-7.6 ± 0.2
$BRET^2_{max}$ ± S.E.M.	0.06 ± 0.01 α	0.025 ± 0.003 α	0.01 ± 0.001
ERK1/2 phosphorylation			
N	4	4	6
EC_{50} (nM)	2	3	ND
pEC_{50} ± S.E.M.	-8.9 ± 0.1	-8.5 ± 0.1	ND
E_{max} ± S.E.M.	368 ± 32	293 ± 32	ND

α□ □ □oretical value, experimental curves did not reach saturation
ND: not detectable

Molecular Pharmacology Fast Forward. Published on August 10, 2016 as DOI: 10.1124/mol.116.105502
This article has not been copyedited and formatted. The final version may differ from this version.

Table 2. Fitted curve parameters of CXCR3 (acceptor) / β-arrestin (donor) titration curves. $BRET_{50}$ and BRET maximal values are given in absolute units. Errors are presented as ± S.E.M.

	Receptor variant			
	CXCR3A-GFP10		**CXCR3B-GFP10**	
	Basal	**CXCL11 (100nM)**	**Basal**	**CXCL11 (100nM)**
β-Arrestin2-Rluc3				
N	4	4	3	3
$BRET_{50}$ ± S.E.M	24 ± 5	5 ± 1	9.5 ± 0.4	7.9 ± 0.3
$BRET_{Max}$ ± S.E.M	0.08 ± 0.001	0.13 ±0.01	0.024 ± 0.002	0.036 ±0.001
β-Arrestin1-Rluc3				
N	4	4	3	3
$BRET_{50}$ ± S.E.M	47 ± 12	2 ± 1	ND	9 ± 3
$BRET_{Max}$ ± S.E.M	0.034 ± 0.002	0.07 ± 0.01	ND	0.023 ± 0.001

Molecular Pharmacology Fast Forward. Published on August 10, 2016 as DOI: 10.1124/mol.116.105502
This article has not been copyedited and formatted. The final version may differ from this version.

Table 3. Summary of CXCR3 variant activated signaling pathways following stimulation with chemokines.

	CXCR3A	CXCR3B	CXCR3Alt
Gαi activation	CXCL11, CXCL10	CXCL11*	ND
β-arrestin2 recruitment	CXCL11, CXCL10 CXCL9□, CXCL4 □	CXCL11	ND
β-arrestin1 recruitment	CXCL11 , CXCL10	CXCL11	ND
Internalization	CXCL11, CXCL10, CXCL9, CXCL4	CXCL11, CXCL10, CXCL9, CXCL4	CXCL11, CXCL9, CXCL4
ERK1/2 phosphorylation	CXCL11, CXCL10, CXCL9□	CXCL11, CXCL9, CXCL4 □	CXCL11, CXCL10□ CXCL9 □

** Only measureable at 100nM chemokine*
□ Weak but statistically significant response
ND: not detectable

Molecular Pharmacology Fast Forward. Published on August 10, 2016 as DOI: 10.1124/mol.116.105502
This article has not been copyedited and formatted. The final version may differ from this version.

Figure 1

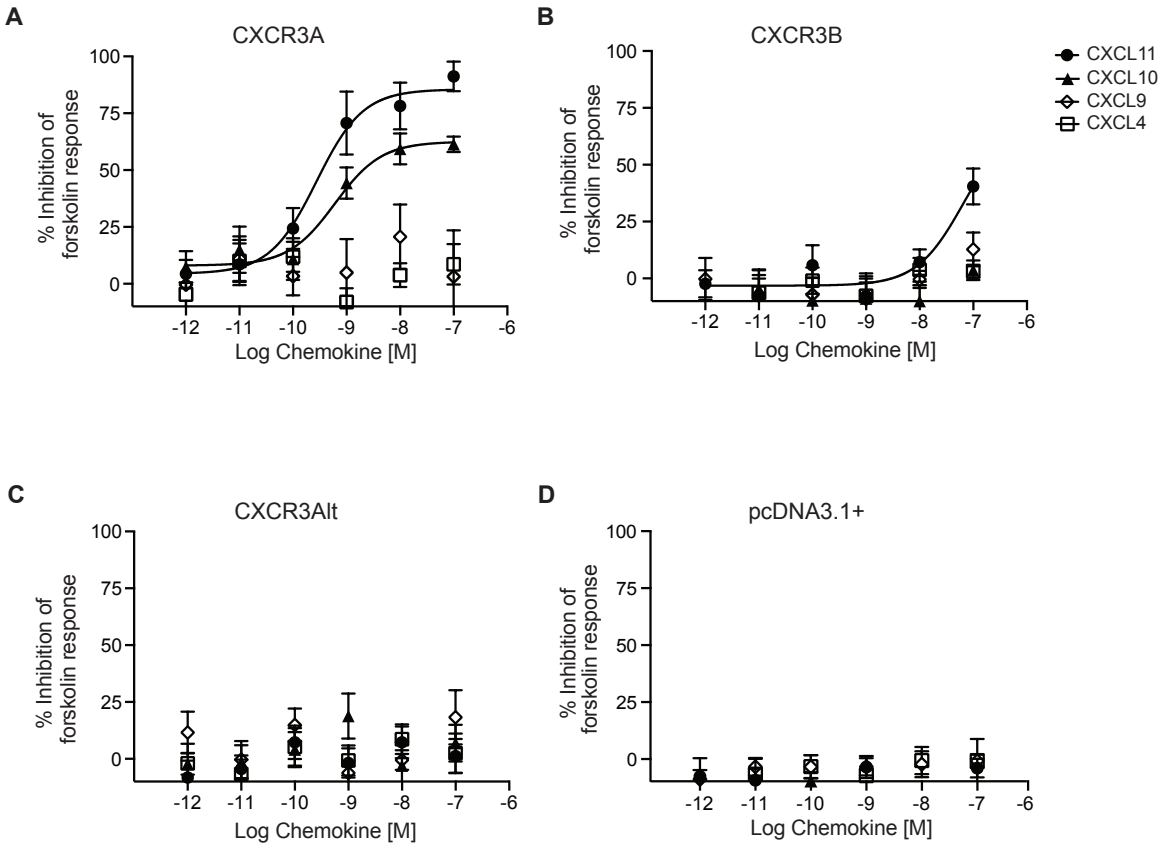

Molecular Pharmacology Fast Forward. Published on August 10, 2016 as DOI: 10.1124/mol.116.105502
This article has not been copyedited and formatted. The final version may differ from this version.

Figure 2

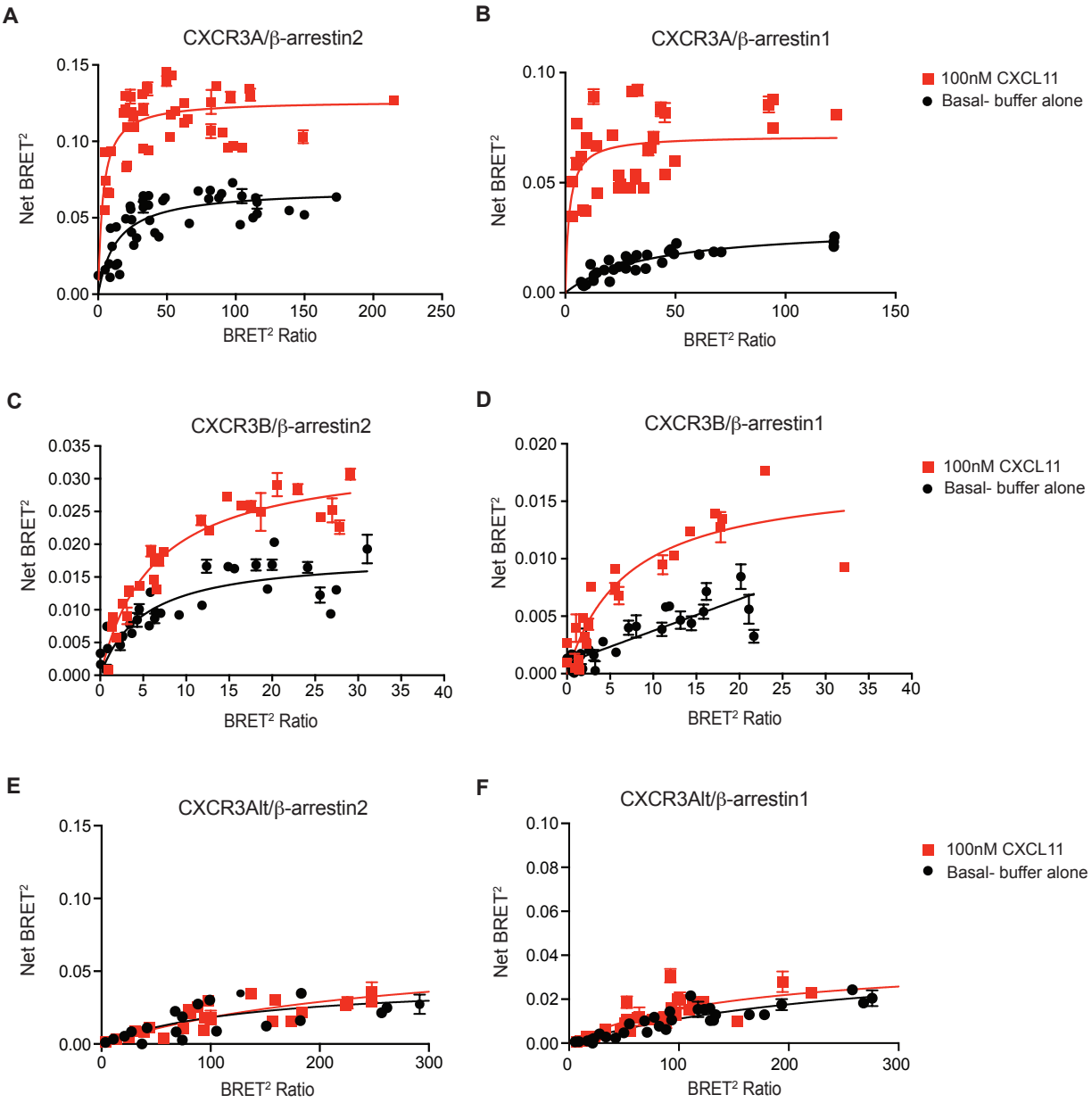

Molecular Pharmacology Fast Forward. Published on August 10, 2016 as DOI: 10.1124/mol.116.105502
This article has not been copyedited and formatted. The final version may differ from this version.

Figure 3

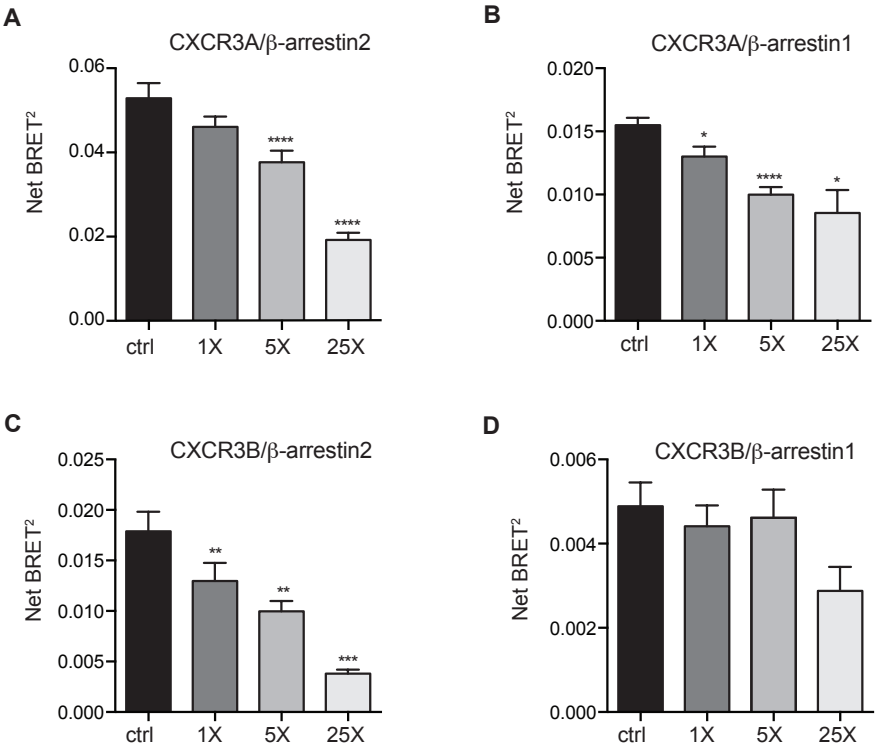

Molecular Pharmacology Fast Forward. Published on August 10, 2016 as DOI: 10.1124/mol.116.105502
This article has not been copyedited and formatted. The final version may differ from this version.

Figure 4

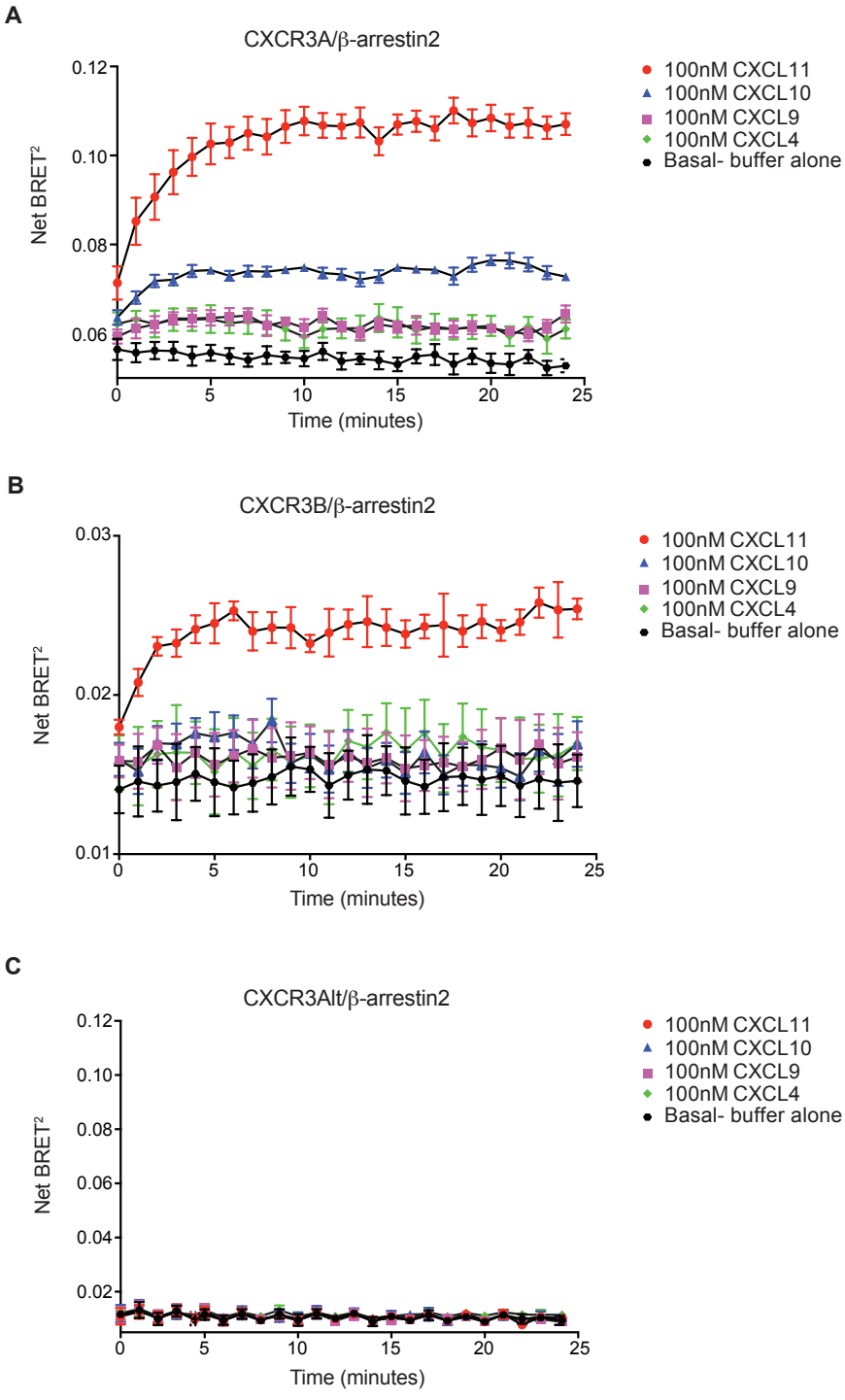

Molecular Pharmacology Fast Forward. Published on August 10, 2016 as DOI: 10.1124/mol.116.105502
This article has not been copyedited and formatted. The final version may differ from this version.

Figure 5

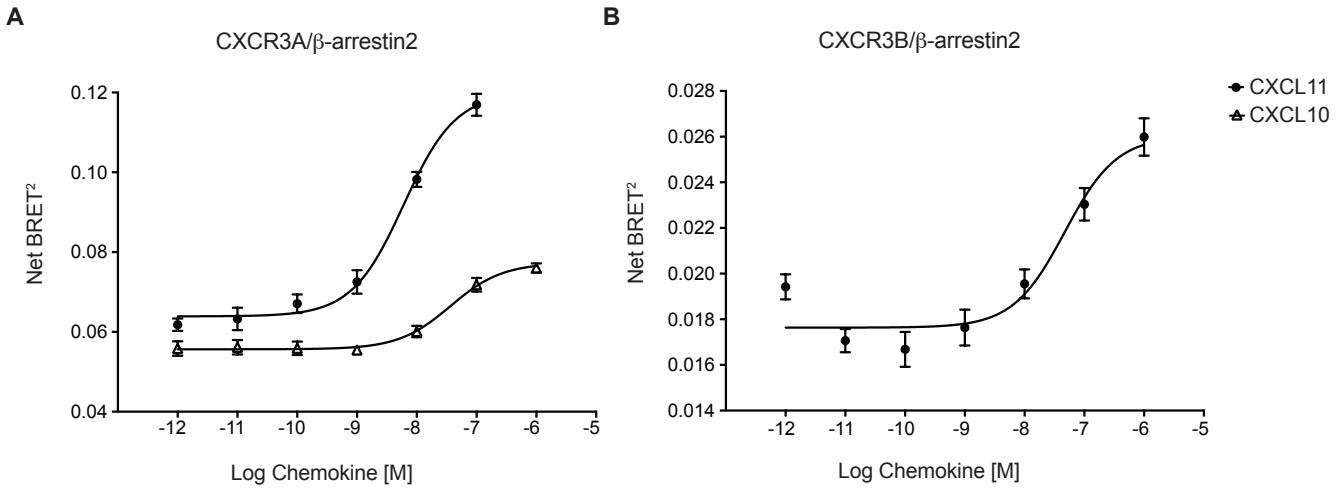

Molecular Pharmacology Fast Forward. Published on August 10, 2016 as DOI: 10.1124/mol.116.105502
This article has not been copyedited and formatted. The final version may differ from this version.

Figure 6

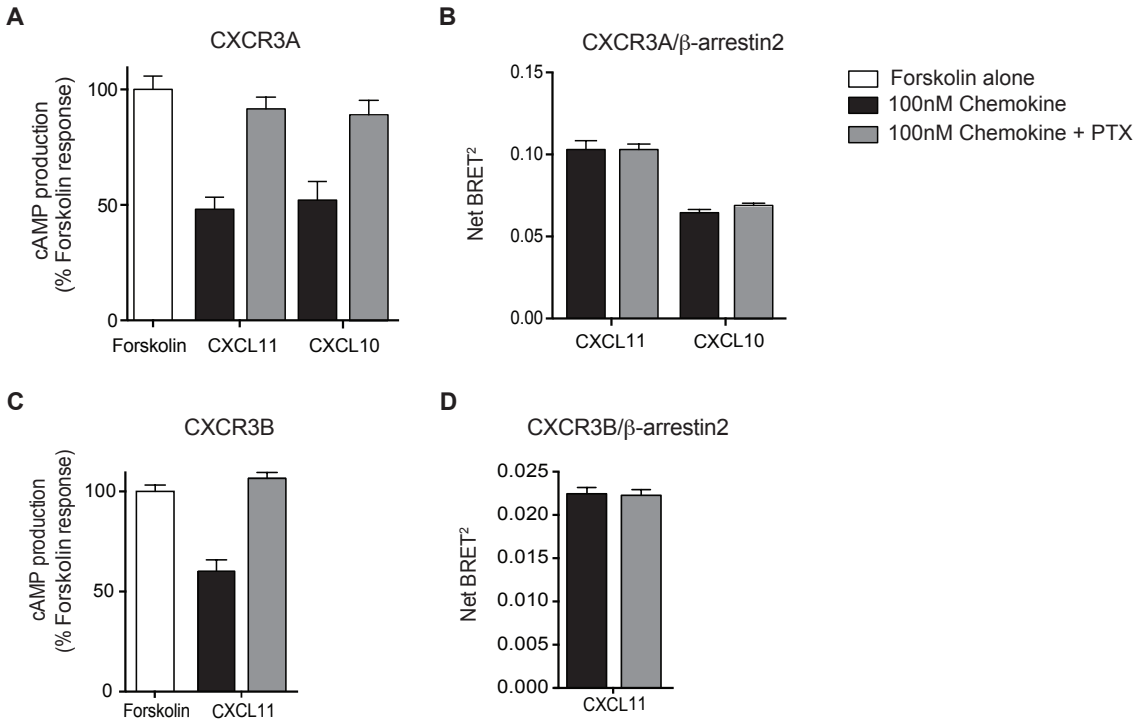

Molecular Pharmacology Fast Forward. Published on August 10, 2016 as DOI: 10.1124/mol.116.105502
This article has not been copyedited and formatted. The final version may differ from this version.

Figure 7

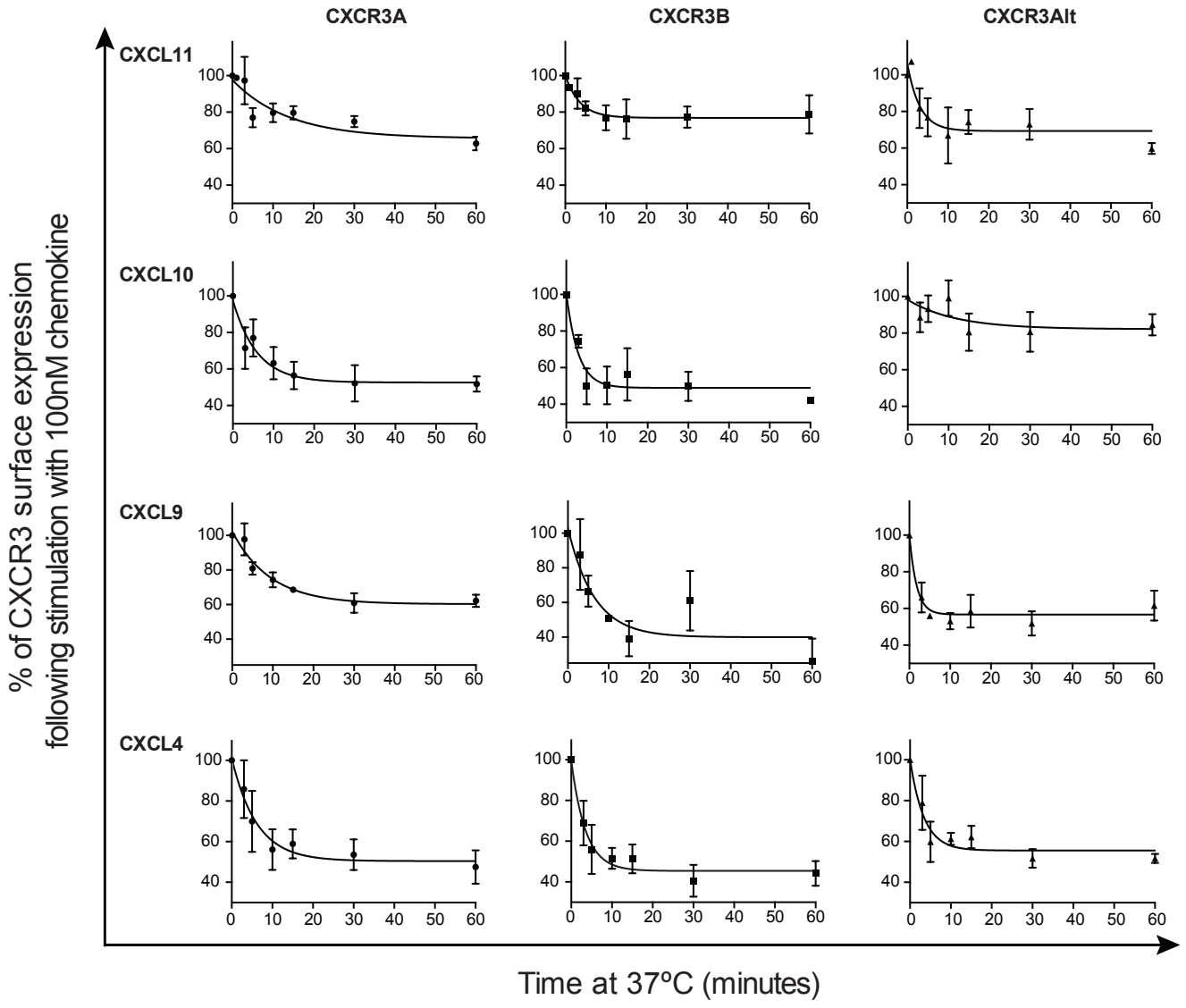

Molecular Pharmacology Fast Forward. Published on August 10, 2016 as DOI: 10.1124/mol.116.105502
This article has not been copyedited and formatted. The final version may differ from this version.

Figure 8